Published in final edited form as:

Circulation. 2018 October 23; 138(17): 1850–1863. doi:10.1161/CIRCULATIONAHA.117.031702.

Deletion of Macrophage Low-Density Lipoprotein Receptor-Related Protein 1 (LRP1) Accelerates Atherosclerosis Regression and Increases CCR7 Expression in Plaque Macrophages

Paul A. Mueller, PhD[1,*], **Lin Zhu, PhD**[2,3,4,*], **Hagai Tavori, PhD**[1], **Katherine Huynh, BS**[1], **Ilaria Giunzioni, PhD**[1], **John M. Stafford, MD, PhD**[3,4], **MacRae F. Linton, MD**[2], and **Sergio Fazio, MD, PhD**[1]

[1]Center for Preventive Cardiology, Knight Cardiovascular Institute, Oregon Health & Science University, Portland, OR;

[2]Division of Cardiovascular Medicine, Vanderbilt University Medical Center, Nashville, TN;

[3]Division of Diabetes, Metabolism and Endocrinology, Department of Medicine, Vanderbilt University Medical Center, Nashville, TN;

[4]Tennessee Valley Healthcare System, Nashville, TN

Abstract

Background——We previously showed that mice lacking LDL receptor-related protein 1 in macrophages (MΦLRP1$^{-/-}$) undergo accelerated atherosclerotic plaque formation due to changes in macrophages including increased apoptosis, decreased efferocytosis, and exaggerated transition to the inflammatory M1 phenotype. Here we sought to explore the role of macrophage LRP1 during regression of atherosclerosis since regressing plaques are characterized by transitioning of macrophages to M2 status as inflammation resolves.

Methods——ApoE$^{-/-}$ mice on a high-fat diet for 12 weeks were reconstituted with bone marrow from apoE-producing wildtype (WT) or MΦLRP1$^{-/-}$ mice and then placed on chow diet for 10 weeks (n=9–11 mice/group). A cohort of apoE$^{-/-}$ mice reconstituted with apoE$^{-/-}$ bone marrow served as baseline controls (n=9).

Results——Plaques of both WT and MΦLRP1$^{-/-}$ bone marrow recipients regressed compared with controls (11% and 22%, respectively; $p<0.05$), and plaques of MΦLRP1$^{-/-}$ recipients were 13% smaller than those of WT recipients ($p<0.05$). Recipients of MΦLRP1$^{-/-}$ marrow had 36% fewer M1 macrophages ($p<0.01$) and 2.5-fold more CCR7^{+} macrophages in the plaque relative to WT mice ($p<0.01$). Additionally, *in vivo* studies of cellular egress showed a 4.6-fold increase in EdU-labeled CCR7^{+} macrophages in mediastinal lymph nodes. Finally, *in vivo* studies of reverse

Address for Correspondence: Sergio Fazio, MD, PhD, Oregon Health & Science University, 3181 Sam Jackson Park Road, HRC 5N, Portland, OR 97239, Tel: 503-494-1775, fazio@ohsu.edu, First Author Twitter Handle: @Paul_A_Mueller.

*P.A.M. and L.Z contributed equally to this work.

Disclosures

None

cholesterol transport (RCT) showed a 1.4-fold higher RCT in MΦLRP1$^{-/-}$ recipient mice ($p<0.01$).

Conclusions——Absence of macrophage LRP1 unexpectedly accelerates atherosclerosis regression, enhances RCT, and increases expression of the motility receptor CCR7 which drives macrophage egress from lesions.

Keywords

atherosclerosis; mouse models; inflammation; low-density lipoprotein receptor-related protein 1; macrophages; atherosclerosis regression

Introduction

Fatty streaks in fetal and infant human aortas are known to decline in subsequent years[1,2] suggesting that the atherosclerotic plaque may undergo bulk regression. However, GLAGOV trial recently showed that extreme LDL-cholesterol (LDL-c) lowering (to <39 mg/dl) for 76 weeks does not produce bulk plaque regression (<1% atheroma volume reduction vs. comparator group)[3]. Thus, regression of atherosclerotic plaques in adults may require more than merely controlling LDL-c, and novel therapies are needed that target specific mechanisms of regression. Of the components of the atherosclerotic plaques, lipids and macrophages are the most amenable to exit it and thus contribute to plaque shrinkage. Regression and stabilization of atherosclerosis has been achieved in mouse models via correction of dyslipidemia[4–6]. The underlying mechanisms include decreased arterial wall retention of apoB-containing lipoproteins[7], suppressed monocyte recruitment[8], efflux of cholesterol from plaques[7,9], and egress of macrophages out of the plaque[10–12]. Although inflammation plays critical roles during atherosclerosis progression, the role of inflammatory macrophages during atherosclerosis regression has not been well studied.

Plaque macrophages undergo differentiation to a functional spectrum book-ended by the complete Ml (inflammatory) and M2 (anti-inflammatory) phenotypes[13]. Progression of atherosclerosis is characterized by a low M2:M1 macrophage ratio in the plaque, accompanied by enhanced production of inflammatory cytokines and matrix metalloproteinases[14,15]. On the other hand, as dyslipidemia resolves, regression of atherosclerotic plaques coincides with decreased macrophage cellularity and a higher M2:M1 ratio[16]. One mechanism for decreased macrophage cellularity in plaques undergoing regression is increased macrophage egress via CCR7 and its ligands CCL19 and CCL21 into the draining lymph nodes[12,17]. However, in an adenoviral-mediated apoE complementation model of plaque regression, reduced monocyte infiltration, not CCR7-dependent egress, was the mechanism behind decreased macrophage cellularity[8].

LRPl is a 600-kDa multi-ligand receptor, which also binds apoE on incoming triglyceride-rich remnants in the hepatic sinusoid[18–20]. Deletion of macrophage LRP1 in mouse models of atherosclerosis results in accelerated plaque growth due to: l) enhanced macrophage apoptosis via suppressed AKT activation, 2) decreased efferocytosis and 3) exaggerated necrosis[21,22]. Macrophage LRP1 is critical for efferocytosis to the point that its deletion negates the anti-atherosclerotic benefits of anti-TNFa inhibitor adalimumab[23]. Macrophages

lacking LRP1 up-regulate secretion of the inflammatory cytokines TNFα, MCP-1, and MMP9[21,22]. Although macrophage LRP1 is clearly protective during atherosclerosis progression, its role during atherosclerosis regression is unknown and this can be used to identify unique differences between these two opposite stages of plaque biogenesis.

We sought to explore the role of macrophage LRP1 during regression of atherosclerosis by placing apoE$^{-/-}$ mice on a high-fat diet for 12 weeks, then reconstituting their bone marrow using wildtype (WT) or MΦLRP1$^{-/-}$ mice as donors, and finally switching them back to chow diet for 10 weeks. ApoE$^{-/-}$ mice reconstituted with apoE$^{-/-}$ marrow served as controls for baseline plaque analyses. Our results show that the lack of LRP1 expression in macrophages unexpectedly promotes atherosclerosis regression. Mice with macrophages lacking LRP1 showed less M1 macrophages in the plaque and increased CCR7-dependent egress of macrophages from the plaque. Thus, loss of macrophage LRP1 has a dual and opposite effect on plaque biogenesis depending on whether the plaque is growing or shrinking.

Materials and Methods

The data that support the findings of this study are available from the corresponding author upon reasonable request.

Study design

8-week-old female apoE$^{-/-}$ mice were fed a western-type diet (42% kcal from fat, Harlan) for 12 weeks followed by lethal irradiation (900rad) and transplantation with bone marrow from WT, MΦLRP1$^{-/-}$, apoE$^{-/-}$, and apoE$^{-/-}$/MΦLRP1$^{-/-}$ (DKO) mice. After bone marrow transplantation (BMT), mice were placed on chow diet. ApoE$^{-/-}$ recipient mice transplanted with apoE$^{-/-}$ bone marrow were sacrificed 2 weeks post-BMT for determination of baseline aortic atherosclerosis (n=9). Ten weeks after BMT, one cohort of mice (n=9–13 for each donor genotype) was euthanized for serum lipid levels and atherosclerosis analyses as described before[21,24]. A second cohort of BMT mice (n=6–8) was studied for *in* reverse cholesterol transport (RCT). A third cohort of BMT mice (n=4–5) was used to label CD11b+ monocytes with 5'-ethynyl-2'- deoxyuridine (Edu) to measure macrophage egress during atherosclerosis regression. A fourth cohort of BMT mice (n=3–4) was used to determine monocyte recruitment. Animal care and experimental procedures were performed according to the regulation of the Institutional Animal Care and Usage Committee of Vanderbilt University and of Oregon Health & Science University.

Atherosclerosis analysis

Frozen sections (10μm) of aortic root were stained with Oil Red O as previously described 24. Images of Oil Red O staining were analyzed using the KS300 imaging system (Kontron Elektronik GmbH).

VLDL, LDL and HDL were separated from pooled serum (pooled from 2–3 mice) using fast performance liquid chromatography (FPLC). Cholesterol and triglyceride levels from serum and FPLC fractions were determined by enzymatic colorimetric assays using colorimetric

kits (Cholesterol Reagent and Triglycerides GPO Reagent kits from Raichem, San Diego, CA).

Western blots

Two microliters of pooled serum, 10μL of FPLC fractions (peak for VLDL or HDL) or 30μg of whole cell lysate (protein concentrations determined via BCA Assay; Bio-Rad) was denatured in sample buffer (Invitrogen) containing reducing buffer (Invitrogen), phospholipase inhibitors and protease inhibitors (Sigma). Proteins were separated with gel electrophoresis and subsequently transferred to PVDF membranes. Membranes were incubated with primary antibody (1:1000) at 4°C overnight and with secondary antibody (1:10000) at room temperature for 1 hour. Antimouse apoB antibody was from Lifespan Biosciences (LS-C20729), anti-mouse apoE antibody was from Abcam (ab20874) and rabbit anti-LRPl was from abcam (ab9255). IRDye 800CW goat anti-rabbit IgG was from LI-COR Biosciences (926–32211).

Quantification of CCR7^{+} macrophages, Ml and M2 macrophage phenotypes, LRP1, Apoptosis, efferocytosis and necrosis in atherosclerotic plaques

Serial cryosections (5μη) of the aortic root were used as described previously[21,24]. Two sequential cryo-sections on the same glass slide were used for each staining to quantify M1 and M2 macrophages in atherosclerotic plaques. One section was stained for M2 marker arginase-1 (Arg1; Gene Tex) and CD68 (Calbiochem), the other section was stained for M1 marker arginase-2 (Arg2; Proteintech Group) and CD68. Briefly, sections were fixed in cold acetone for 10 minutes, washed twice with PBS, blocked in background buster (Innovex) at 37°C for 1 hour, and incubated with primary antibodies at 4°C overnight. Sections were then washed with PBS 3 times, incubated with Alexa Fluor 594 anti-rabbit IgG (Invitrogen) and streptavidin Alexa Fluor 488 (Life technologies) at 37°C for 1 hour. Anti-mouse CCR7 antibody was from BD sciences. Images were captured using Olympus 1X81 microscope and analyzed using Adobe Photoshop CC (Mac) software. For quantification of M2 or M1 macrophages, Arg1^{+} or Arg2^{+} (red) and CD68 (green) double positive cells were visualized with separated color channel filter using Adobe Photoshop CC (Mac) software.

Studies of LRP1 expression in baseline and regressing plaques was performed according to the established protocol described above and using anti-rabbit LRP1 (Abcam) and anti-rat Mac2 (Abcam).

Apoptosis was quantitated in serial cryosections (5μm thickness) from control,WT, and MΦLRP1$^{-/-}$ recipient mice undergoing regression using the *In Situ* Cell Death Detection Kit from Roche according to the manufacturer's instructions. Macrophages were labelled with a Mac-2 antibody (Abcam) and efferocytosis was determined by quantifying TUNEL area within Mac-2 labelled macrophages. Necrosis in atherosclerotic plaques was quantitated by measuring the Harris's hematoxylin and eosin staining (H&E) negative cellular area in the intima versus total intimal area using the method described previously[24].

In vitro cholesterol efflux

Peritoneal macrophages were collected from WT, MΦLRP1$^{-/-}$, ApoE$^{-/-}$ and DKO mice 72 hours after i.p injection of 3% thioglycollate. Cells were washed twice with phosphate buffered saline (PBS) and seeded onto 24-well plates (5×10^5 cells/well). After 2 hours, non-adherent cells were removed, and plates washed with PBS twice. Cells were loaded with 3uCi/ml 1,2-^{3}H-cholesterol with acetylated LDL (250ug/ml; Alfa Aesar). 48 hours later, media was removed, and cells were washed twice with PBS. Cells were equilibrated in DMEM with 0.25% BSA containing interferon gamma (IFNγ, 50ng/ml, Peprotech) in DMEM overnight. The remaining cells were induced for M2 polarization using IL4 (25ng/ml, Sigma) or M1 polarization by IFNγ (50ng/ml, Peprotech) and LPS (100ng/ml, Sigma) in DMEM with 0.25% BSA for 3 hours. T0 cells were cultured in DMEM with 0.25% BSA containing IFNy (50ng/ml) for the same amount of time (3 hours). After 3 hours, Time-0 cells (T0) were washed twice with PBS, air dried and stored at −20°C. The remaining cells were washed twice with PBS. Then cells are treated with freshly prepared M1 or M2 polarization media containing A poA 1(50 ug/ml, Sinobiological Inc) for cholesterol efflux for 24 hours. 120μ1 of media from each well was collected and transferred directly to multiscreen filter plate (Millipore). 100μ1 of media was used for radioactivity determination by liquid scintillation counting (LSC).

In vivo reverse cholesterol transport assay

The *in vivo* RCT assay was modified from an established model by Tanigawa et al[25]. Briefly, peritoneal macrophages from WT, MΦLR1$^{-/-}$, apoE$^{-/-}$, and DKO mice were collected 72 hours after intraperitoneal injection of thioglycollate. Macrophages were first cultured in DMEM with 10% FBS for 2 hours. After cell attachment to plastic media was switched to DMEM with 0.2% BSA overnight. Macrophages were labeled with 3 μCi/mL ^{3}H-cholesterol enriched with 50μg/ml of acetylated LDL for 48 hours to generate 3H-cholesterol loaded foam cells. Labeled foam cells were washed twice, equilibrated in medium with 0.2% BSA for 6 hours, centrifuged, and resuspended in phenol red-free RPMI medium immediately before use. BMT mice on chow diet, as described earlier, received intraperitoneal injections of labeled foam cells of the same genotype and fed chow diet ad libitum. After 48 hours, mice were euthanized, blood was collected by cardiac puncture, gallbladder separated, and the liver removed and flash frozen for lipid extraction. Feces were collected until mice were euthanized.

Serum and liver lipids were extracted as described before[26]. The lipid layer was collected, evaporated and resuspended for scintillation counting. The gallbladder was lysed in 0.1N NaOH for 4 hours and subjected for scintillation counting. Feces were soaked in 50mL of 0.1N NaOH overnight at 4°C and then homogenized.1mL of the homogenized feces was subjected to scintillation counting.

In vivo labeling of bone marrow with Edu, isolation of CD11b$^+$monocytes, and evaluation of cell emigration into adjacent lymph nodes during regression

Bone marrow was isolated from 7-week-old female wildtype, MΦLR1$^{-/-}$, apoE$^{-/-}$ and DKO mice after two weeks intraperitoneal injection of Edu (100μg per mouse twice a week, each injection followed a 100μ1 bleeding from suborbital vein). CD11b$^+$ monocytes were isolated

from fresh bone marrow using CD11b MicroBeads (MACS) according to the manufacturers protocol. Briefly, bone marrow was collected in RPMI phenol red-free medium with 2% FBS and 5UI/mL heparin. Bone marrow was washed twice with RPMI supplemented with 2% FBS and then were resuspended in 0.5% BSA, 2mM EDTA in 1X PBS. Cells were diluted to 1×10^7 cells/90μL. 10μL of CD11b MicroBeads were added for every 1×10^7 bone marrow cells. Cells were incubated for 15 minutes on ice, washed, resuspended and retained in the MACS LS Columns in the magnetic field of a SuperMACS separator at 4°C. After the magnetic separation, the columns were washed, removed from the magnetic field, and dispensed into 15mL sterile tubes using 5mL buffer and firmly applying the supplied plunger.

A small portion of each genotype's cells was used to determine cell population using flow-cytometric analysis, and more than 98% cells were CD11b positive. The remaining cells were resuspended in phenol red-free and serum free RPMI medium. Cells were injected into the 3rd cohort of BMT mice of their respective genotype through suborbital veins. Seventy-two hours following suborbital injections the mice were sacrificed. Blood and mediastinal lymph nodes were collected to evaluate the emigration of Edu labeled $CCR7^+$ cells from plaque using flow-cytometry. Superficial cervical lymph nodes were used as negative controls. Lymphocytes were isolated using cell strainers (70μm Nylon, Falcon). Click-iT® Edu Flow Cytometry Assay Kits (Invitrogen, Pacific Blue™ azide, Cat. No. C10418) were used for the detection of Edu. For detection of CCR7 expression, PE conjugated anti-mouse CD 197 (CCR7) monoclonal antibody (BD Biosciences, Cat. 560682) was used.

In vitro analysis of gene and protein expression in polarized macrophages

Peritoneal macrophages were collected from WT and $M\Phi LRP1^{-/-}$ mice ($n\geq6$), 3 days after i.p. injection with 3% thioglycollate and seeded in 6-well plates at 3×10^6 cells/well in DMEM with 10% FBS. 4 hours later, floating cells were removed and attached cells were washed twice with 1X PBS. Cells were cultured in DMEM with 1% BSA overnight for macrophage synchronization. Macrophages were primed for 6–8 hours in DMEM with 0.1% FBS containing IFNγ (50ng/mL). To generate M1 macrophages, primed macrophages (Mo) were treated with IFNγ (50ng/mL) and LPS (100ng/mL) for 12 hours. To generate M2 macrophages, primed macrophages were treated with IL4 (25ng/mL) for 12 hours. For M1 to M2 switching, M1 macrophages were generated as described above and then treated with IL4 (25ng/mL) for 12 hours to switch them to the M2 phenotype. RNA was extracted using TRIzol according to the manufacturer's protocol. *Abcal, Abcgl, Srb1, LrpI, Srebfl, Srebf2, Ccr7, Rpl32* and 18s primers were from ThermoFisher and real-time PCR was performed using Applied Biosystems ViiA7. Experiments were performed in triplicate and repeated three times.

Human monocyte THP-1 cells (ATCC) were differentiated to macrophages with phorbol 12-myristate 13-acetate (10ng/mL; Sigma Aldrich) treatment for 48 hours. After 48 hours, PMA-treated THP-1 cells were treated with IFNγ and LPS or IL4 to generate Ml and M2 macrophages as described above.

In vivo monocyte recruitment

Bone marrow was isolated from 7-week-old male WT, MΦLRPl$^{-/-}$ donor mice. CD11b^{+} monocytes were isolated from fresh bone marrow using CD11b MicroBeads (MACS) according to the manufacturers protocol and as described above. CD11lb monocytes were labeled with CMFDA Green Cell Tracker (ThermoFisher) and resuspended in phenol red-free and serum free RPMI medium. 2.0×10^{6} labelled CD11b+ monocytes were i.v. injected into recipient mice of their respective genotype undergoing regression. 72 hours after injections, mice were sacrificed and aortic root serial cryosections (5μm) were stained for CD68 and DAPI. Monocyte recruitment was determined by counting newly recruited monocyte/macrophages positive for CD68 and normalized to lesion area.

Statistical Analyses

Shapiro-Wilk normality test (alpha=0.05) was used to determine whether sample group data was distributed normally. For images, data was collected from at least two sections for each mouse and averaged, and none of the experimental mice were excluded from the analysis. Data are expressed as mean ± SD unless otherwise stated. For comparison of two groups we performed a Student's t-test. For comparison among genotypes (including baseline or before BMT) we used one-way ANOVA analysis with Bonferroni's post hoc test unless stated otherwise. For gene expression analyses, when evaluating the median fold change in gene expression in differentiated macrophage subtypes (Ml and M2) relative to primed Mo we performed a Wilcoxon Signed Rank test on the fold changes of M1 vs. Mo and M2 vs. Mo as non-parametric one-sample test of the null hypothesis that the median fold change is equal to one. For cholesterol efflux and gene expression comparing effects across genotypes and macrophage subtypes we used two-way ANOVA with Sidak's multiple comparisons test. To assess differences across genotypes of Edu^{+}/CCR7^{+} double-positive cell counts in mediastinal and superficial cervical control lymph nodes we performed an ANCOVA using donor genotype as the independent variable and the paired-superficial cervical control samples as the covariate. Tukey's post hoc test was then used to report pairwise differences in mediastinal lymph nodes. Where sample size was too low or did not qualify for parametric statistics, we performed an unpaired Mann-Whitney to determine differences between groups of two and Kruskal-Wallis using Dunn's post hoc test was used for multiple groups. $p<0.05$ was considered significant.

Results

Bone marrow-m ediated apoE complementation corrects hyperlipidemia in apoE$^{-/-}$ mice

We previously demonstrated that transplanting bone marrow from apoE$^{+/+}$ mice into apoE$^{-/-}$ recipients corrects their hypercholesterolemia and prevents atherosclerosis through the re-introduction of apoE both in plasma and in the plaque[27]. Others have shown that adenoviral-mediated reintroduction of apoE into apoE$^{-/-}$ mice induces atherosclerosis regression[8]. Thus, to determine whether bone marrow-mediated apoE complementation is sufficient to correct hyperlipidemia and induce regression we performed BMT on apoE$^{-/-}$ mice fed high fat diet for 12 weeks using wildtype (WT), MΦLRP1$^{-/-}$, apoE$^{-/-}$, and apoE$^{-/-}$/ MΦLRP1$^{-/-}$ (DKO) mice as marrow donors, and then placed the recipient mice on chow diet for 10 weeks. Serum was separated by FPLC and cholesterol levels were determined to track the

different lipoprotein fractions (Fig 1A). Area-under-the-curve analyses of cholesterol fractions showed a 50% decrease in VLDL/LDL cholesterol levels in both apoE$^{-/-}$ and DKO recipients compared with pre-BMT levels (Fig S1A and B; grey and open bars). These lipid changes were attributable to return to chow diet. However, in WT and MΦLRP1$^{-/-}$ recipient mice the corresponding decrease was 94% and 80% for VLDL and LDL, respectively (Fig S1A and B; red and blue bars). This was due to the reintroduction of apoE, which has a strong hypolipidemic effect, and to the return to chow diet. Interestingly, HDL was 1.9-fold higher in MΦLRP1$^{-/-}$ recipient mice compared to WT recipients (Fig S1C). Immunoblots of serum from both WT and MΦLR1$^{-/-}$ recipient mice showed presence of apoE and decreased apoB100 levels compared to pre-BMT analyses (Fig 1B).

Expression of LRP1 in atherosclerosis regression

We evaluated the expression of LRP1 in atherosclerotic plaques in apoE$^{-/-}$ recipient mice sacrificed 2 weeks after BMT (baseline) and in WT recipient mice undergoing regression for 10 weeks on chow diet. Intraplaque LRP1 decreased in WT recipient mice during regression compared to baseline controls (Fig 2A). Regressing plaques are known for having increased M2 vs. M1 macrophages[15, 28]. Thus, we compared *Lrpl* gene expression in mouse peritoneal macrophages (MPMs) from WT mice polarized to either the inflammatory M1 phenotype using interferon gamma (IFNγ) or the anti -inflammatory M2 phenotype with interleukin-4 (IL4). *Lrpl* was 3-fold higher in M1 macrophages compared to M2 ($p<0.05$) (Fig 2B). To determine whether elevated Lrp1 gene expression in the inflammatory M1 state was specific to mice we treated human THP-1 monocytes with phorbol 12-myristate 13-acetate (PMA) to differentiated them into macrophages. Differentiated THP-1 cells were then treated with IFNγ and either LPS or IL4 to simulate M1 and M2 macrophages respectively. Interestingly, LRP1 protein levels increased in PMA-treated THP-1 cells compared to naïve THP-1 monocytes (Fig 2C left panel). We also observed sustained LRP1 level increases in THP-1 macrophages treated with IFNγ and LPS, and complete ablation of LRP1 protein in cells treated with IL4 (Fig 2C right panel).

Loss of M acrophage LRP1 Accelerates Plaque Regression

We evaluated atherosclerosis in WT and MΦLRP1$^{-/-}$ recipient mice after 10 weeks on chow diet to determine the role of macrophage LRP1 during regression. A cohort of apoE$^{-/-}$ recipient mice was sacrificed 2 weeks after BMT to serve as baseline controls. Serum cholesterol was 866±85 mg/dL before BMT and decreased by 82% in WT recipients (157±36 mg/dL; $p<0.0001$) and by 84% in MΦLR1$^{-/-}$ recipient mice (140±33 mg/dL; $p<0.0001$) (Fig 3A). Serum triglycerides were 108±33 mg/dL before BMT and decreased by 44% in WT recipients (61±16 mg/dL; $p<0.01$) and by 50% in MΦLR1$^{-/-}$ recipient mice (54±17 mg/dL; $p<0.001$) (Fig 3B). There was no difference in total serum cholesterol or triglycerides between WT and MΦLR1$^{-/-}$ recipients. Relative to baseline controls (645± 60×10^3 μm^2), aortic sinus plaque area decreased 11% in WT (576±40×10^3 μm^2; $p<0.05$) and 22% in MΦLR1$^{-/-}$ recipient mice (503±53×10^3 μm^2; $p<0.0001$). Aortic sinus plaque area was 13% smaller in MΦLR1$^{-/-}$ recipient mice compared to WT recipients ($p<0.05$) (Fig 3C and D).

Macrophage LRP1 is protective during the progression of atherosclerosis in part due to its role in limiting apoptosis and accelerating efferocytosis[22, 24]. Cryosections from baseline, WT and MΦLRP1$^{-/-}$ recipient mice were stained for TUNEL to evaluate the levels of intraplaque apoptosis. There was no change in levels of apoptosis among baseline controls and mice undergoing regression (Fig S2A and B). We also determined the degree of efferocytosis in lesions by comparing TUNEL^{+} area within macrophages stained with Mac-2. Again, no differences were observed across the groups (Fig S2C). Coinciding with these observations, no differences in necrotic core area were observed between groups (Fig S2D).

ApoE$^{-/-}$ and DKO recipient mice did not undergo regression after 10 weeks on chow diet (Fig S3C and D). However, apoE$^{-/-}$ recipient mice developed significantly larger necrotic cores compared to baseline (Fig S2E).

Loss of M acrophage LRP1 increases reverse cholesterol transport during atherosclerosis regression

Net efflux of cholesterol from plaques to the liver and its excretion through feces, a process known as reverse cholesterol transport (RCT), are putative mechanisms of atheroma regression. To determine RCT *in vivo*, we injected WT, MΦLRP1$^{-/-}$, apoE$^{-/-}$, and DKO macrophages loaded with ^{3}H-cholesterol acLDL into the peritoneal cavity of BMT mice of matched donor genotype. Serum, feces, and liver were collected to determine the extent of reverse cholesterol transport, as described in Materials and Methods. All mice that received apoE complementation (recipients of WT and MΦLRP1$^{-/-}$ marrow) demonstrated enhanced RCT in the liver and feces compared to apoE$^{-/-}$ and DKO recipients (Fig 4A–C). Total, liver, and feces RCT in MΦLRP1$^{-/-}$ recipient mice was ~1.4-fold higher than that of WT recipients (Fig 4B–D; $p<0.01$). There were no differences in RCT between apoE$^{-/-}$ and DKO recipient mice.

In macrophages, tyrosine phosphorylation of an NPxY domain in LRP1 initiates a signaling cascade activating PPARγ and LXR to regulate cholesterol homeostasis through the expression of ABCA1[29]. Thus, loss of LRP1 should correlate with reduced ABCA1 expression and diminished cholesterol efflux capacity. To determine whether the enhanced RCT in MΦLRP1$^{-/-}$ recipient mice observed in vivo was due to macrophage cholesterol efflux, we isolated MPMs from WT, MΦLRP1$^{-/-}$, apoE$^{-/-}$, and DKO mice. MPMs were loaded for 48 hours with acetylated LDL containing ^{3}H-cholesterol before being polarized to the M1 or M2 phenotype as described in Materials and Methods. Cholesterol-laden macrophages were exposed to apoA1 for 24 hours to induce cholesterol efflux. While cholesterol efflux from M2 macrophages of MΦLRP1$^{-/-}$ recipient mice was ~1.2-fold higher compared to their M1 counterpart (Fig 4E) we did not observe differences in cholesterol efflux across the other genotypes. We also observed no changes in mRNA expression levels of key cholesterol transport proteins in M1 versus M2 macrophages from WT and MΦLRP1$^{-/-}$ mice (Fig 4F–H).

Loss of M acrophage LRP1 Decreases Plaque M acrophage Content and M1 Cellularity

As mentioned previously, regressing plaques have reduced macrophage content but also a preponderance of M2 vs. M1 macrophages. Arginase 1 and arginase 2 are commonly used as markers for M2 and M1 macrophages, respectively. We evaluated M2 macrophage concentration in regressing plaques and determined that WT recipient mice had 3.4-fold more (63.4±4.2% of total $CD68^+$ cells; $p<0.0001$) and $M\Phi LRP1^{-/-}$ recipient mice had 3.2-fold more M2 macrophages (59.4±8.5% of total $CD68^+$ cells; $p<0.0001$) than baseline controls (18.8±3.5% of total $CD68^+$ cells), (Fig 5A and D). There were no differences in M2 macrophage concentration between WT and $M\Phi LRP1^{-/-}$ recipient mice. We observed the same concentration of M1 macrophages in the plaques of WT recipient mice (47.6±4.1% of total $CD68^+$ cells) as the baseline controls (45±4.3% of total $CD68^+$ cells) whereas $M\Phi LRP1^{-/-}$ recipient mice unexpectedly had an M1 concentration 36% less (28.6±3.7% of total $CD68^+$ cells; $p<0.0001$) (Fig 5B and E). This means that the plaques of $M\Phi LRP1^{-/-}$ recipient mice had 40% fewer M1 macrophages relative to plaques of WT recipient mice ($p<0.0001$) even though the correction of dyslipidemia was similar in these two groups. Plaques from $M\Phi LRP1^{-/-}$ recipient mice harbored a 4-fold higher M2/M1 ratio than baseline controls ($p<0.001$) (Fig 5F). No differences were observed in the M2/M1 phenotype ratio between baseline controls and WT recipients, or between WT and $M\Phi LR1^{-/-}$recipient mice. Compared to baseline controls (172.5±10.1 cells/section) total $CD68^+$ macrophage content decreased 60% in WT recipients (69.7±8.8 cells/section; $p<0.0001$) and 70% in $M\Phi LR1^{-/-}$ recipients (52.33±5.2 cells/section; $p<0.0001$) (Fig 5C). Regressing plaques from $M\Phi LR1^{-/-}$ recipient mice had 25% fewer $CD68^+$ cells than those of their WT recipient counterparts ($p<0.01$).

Plaques from DKO recipient mice, which did not undergo regression, had more M2 and fewer M1 macrophages compared to baseline and $apoE^{-/-}$ recipient mice (Fig S4A–E). Also, DKO recipient mice had a ~4.0-fold higher M2/M1 ratio than both comparator groups (Fig S4F). No differences in total $CD68^+$ macrophages were observed (Fig S4C).

Regressing plaques in $M\Phi LRP1^{-/-}$ recipients show accelerated CCR7-dependent macrophage egress

Another mechanism of atherosclerosis regression is the CCR7-dependent macrophage egress from the plaque[11,12]. We evaluated CCR7 expression in plaque macrophages (Fig 6A–B). Compared to baseline controls (5.8±1.9 cells/section), WT recipient plaques had 2.6-fold more $CCR7^+$ macrophages (15.2±2.1 cells/section; $p<0.01$) and plaques from $M\Phi LR1^{-/-}$ recipient mice had 6.5-fold more than baseline (37.7±5.6 cells/section; $p<0.0001$). Plaques from $M\Phi LRP1^{-/-}$ recipient mice had 2.5-fold more $CCR7^+$ macrophages per section compared to WT recipients ($p<0.0001$). To determine the effect of LRP1 and its loss on plaque macrophage egress *in vivo* we injected EdU-labeled $CD11b^+$ monocytes from WT, $M\Phi LRP1^{-/-}$, $apoE^{-/-}$ or DKO mice into mice of the same donor genotype. After 72 h, lym ph nodes were homogenized and subjected tofACS analysis to quantitate EDU+ CCR7+ cells (Fig S5). Mediastinal lymph nodes (draining from the aorta) of $M\Phi LRP1^{-/-}$ recipient mice contained 4.6-fold more $CCR7^+$ EdU^+ doublepositive cells than did WT recipient controls (3.88±2.2 versus 0.84±0.19% of parental cells; $p<0.05$) (Fig 6C). Mediastinal lymph nodes of $M\Phi LRP1^{-/-}$ recipient mice also contained significantly more double-

positive cells than apoE$^{-/-}$ lymph nodes. CCR7^{+} EdU^{+} double-positive cells found in superficial cervical lymph nodes were negligible. *In vitro*, WT and M OLRPl$^{-/-}$mouse peritoneal macrophages were first primed using IFNγ (Mo) and then polarized to the Ml phenotype (via IFNγ + LPS). A cohort of Ml macrophages was then switched to the M2 phenotype with IL4. *Ccr7* expression was determined using qRT-PCR. Expression of *Ccr7* was increased 5.5-fold in WT Ml macrophages and increased 20-fold in MΦLRPl$^{-/-}$ Ml macrophages compared to their respective Mo control ($p<0.05$) (Fig 6D). Also, MΦLRPl$^{-/-}$ Ml macrophages displayed 2.6-fold higher levels of *Ccr7* than WT Ml counterparts, but this did not reach statistical significance. Feig et al. have shown that the murine CCR7 gene contains binding sites for sterol regulatory element binding proteins (SREBPs), specifically SREB1, and treatment of the murine macrophage cell line RAW264.7 with statins induces *Srebf1* and *Srebf2* expression to upregulate CCR7[30]. Thus, we polarized MPMs from WT and MOLR1$^{-/-}$ mice to the Ml phenotype and measured mRNA expression of *Srebf1* and *Srebf2.* Indeed, Ml macrophages from MΦLRPl$^{-/-}$ mice had a 2-fold increase in *Srebf1* compared to WT Ml macrophages; no differences were observed in *Srebf2* expression (Fig 6E).

To determine whether increased monocyte recruitment to the plaque could explain the increased egress, we labeled CD11b monocytes from WT and M OLRPl$^{-/-}$ donor mice with fluorescent green cell tracker CMFDA and injected 2.0×10^{6} cells into mice of their respective genotype undergoing regression. After 72 h, mice were sacrificed and aortic root cryosections were stained for macrophages using CD68. While plaques from both WT and MΦLRPl$^{-/-}$ recipient mice contained CD68+ CMFDA+ double-positive staining, there was no difference between genotypes (Fig 6F and G).

Discussion

In this study we identify an unexpected role for macrophage LRP1 during atherosclerosis regression in the mouse. We observed decreased LRP1 expression in mouse and human macrophages polarized to an anti-inflammatory state compared to their pro-inflammatory counterpart. We transplanted WT and MΦLR1$^{-/-}$ bone marrow into apoE$^{-/-}$ mice with established plaques, thus reintroducing apoE to correct the hyperlipidemia and drive regression of atherosclerosis. After 10 weeks on the regressive environment, we observed diminished intraplaque LRP1 in WT recipients and that loss of macrophage LRP1 accelerates plaque regression independently of plasma lipid levels. During regression we observed elevated serum apoE and HDL and increased RCT in MΦLR1$^{-/-}$ recipient mice relative to their WT recipient controls. Extensive plaque characterization revealed a reduction in CD68^{+} cell counts and elevated M2/M1 macrophage ratios in MΦLR1$^{-/-}$ recipient mice caused by selective loss of inflammatory M1 macrophages. There were no differences in plaque apoptosis or efferocytosis. Finally, plaques from mice lacking macrophage LRP1 had increased CCR7^{+} macrophage staining, and EDU^{+}/CCR7^{+} double positive macrophages accumulated in nearby mediastinal lymph nodes, not in control lymph nodes, which was independent of monocyte recruitment. In fact, inflammatory M1 macrophages from MΦLRP1$^{-/-}$ mice display increased *Srebfl* gene expression compared to WT M1 controls, a transcription factor directly implicated in CCR7 expression.

Models of atherosclerosis regression, studied in the mouse for nearly two decades[31], rely upon rapid correction of dyslipidemia in animals with established plaques[8, 30, 32]. Key mechanisms driving regression include: 1) increased reverse cholesterol transport[7, 33]; 2) enrichment of anti-inflammatory M2 macrophages; 3) depletion of inflammatory M1 macrophages[15, 16, 28]; 4) upregulated macrophage CCR7 expression and CCR7-dependent egress of resident macrophages from plaques to nearby lymph nodes[12, 17]; and 5) suppressed monocyte infiltration into the atheroma[8]. Daugherty et al. provide detailed recommendations on the design and interpretation of mouse models of atherosclerosis as well as regression[34]. We have developed a model of murine regression using apoE complementation from bone marrow cells (WT and MΦLR1$^{-/-}$ donors) into apoE$^{-/-}$ mice with established plaques. Bone marrow apoE is sufficient to correct dyslipidemia in apoE$^{-/-}$ mice 27 (Figure 1) and to drive regression of atherosclerotic plaques (Figure 3). As observed in other established models of regression, mice in this study demonstrated increased reverse cholesterol transport (Figure 4), enrichment of M2 plaque macrophages (Figure 5), upregulated macrophage CCR7, and increased EDU^{+}/CCR7^{+} macrophage accumulation in mediastinal lymph nodes (Figure 6).

Although there were no differences in plasma lipids between WT and MΦLR1$^{-/-}$ recipient mice, loss of macrophage LRP1 increased serum apoE and HDL-cholesterol levels (Fig 1 and S1). Macrophage-derived apoE is known to have local protective effects on the plaque[35], and thus may have contributed to the inflammation resolution and accelerated regression observed in this study. In fact, previous regression studies have reported a direct correlation between plasma apoE concentration and plaque size[31]. Elevated serum HDL-cholesterol in MΦLRP1$^{-/-}$ recipient mice compared to WT recipient controls may relate to the observed increases in RCT (Fig 4) and to accelerated plaque resolution (Fig 5). Regression has also been achieved in mouse models through HDL-based interventions (i.e., via apoA-I overexpression) promoting RCT from macrophage foam cells[36, 37]. It is unclear why loss of LRP1 in macrophages would directly promote RCT considering that we observed no differences in cholesterol efflux or in the expression of the key cholesterol transport proteins ABCA1, ABCG1 and SRB1 between WT and MΦLR1$^{-/-}$ macrophages (Fig 3E–H). However, previous studies have implicated functional macrophage egress through the lymphatic system as a modulator of RCT[38].

Macrophage clearance from the atherosclerotic plaque is a hallmark of regression. In this study, plaques from MOLR1$^{-/-}$ recipient mice had fewer CD68^{+} cells. Specifically, MΦLRP1$^{-/-}$ recipient mice showed similar numbers of M2 but fewer M1 macrophages than in WT recipient controls, suggesting that M1 cells of MΦLRP1$^{-/-}$ recipient mice undergo enhanced egress, enhanced necrosis, decreased monocyte recruitment or perhaps all three (Figure 5A–E). During progression of atherosclerosis, macrophage LRP1 acts as an efferocytosis receptor for “eat me” signals such as calreticulin. Absence of LRP1 may negate the effects of blocking “don’t eat me” signals such as CD47[39, 40]. However, the lack of differences in monocyte recruitment (Figure 6F and G), apoptosis, necrosis, and efferocytosis in plaques of regressing mice supports a potential role for enhanced egress (Fig S2A–D). Inhibiting CCR7-dependent macrophage egress with blocking antibodies to its ligands CCL19 and CCL21 disrupts plaque regression[12]. A previous study on macrophage chemotaxis reported similar CCR7 protein levels in M1 and M2 macrophages. However, only M1 macrophages responded to CCL19 and CCL21[41]. The CCR7 gene contains binding

sites for the SREBPs in both human and mice and its expression is directly modulated by SREBPs[11]. Interestingly, SREBPs modulate LRP1 expression in human macrophage foam cells[42]. We and others have reported that LRP1$^{-/-}$ macrophages have reduced lipoprotein uptake both *invivo* and *in vitro*[21, 42, 43], a functional consequence that could lead to SREBP activation. These reports, together with our observations of increased CCR7^{+} macrophages in MΦLR1$^{-/-}$ recipient plaques (Fig 6A and B), enhanced accumulation of EdU^{+} CCR7^{+} macrophages in the mediastinal lymph nodes of MΦLRP1$^{-/-}$ recipient mice (Fig 6C and S5), and elevated *Srebf1* gene expression in LRP1$^{-/-}$ M1 macrophages (Fig 6E) suggest that the mechanism of M1 macrophage depletion is a CCR7-dependent egress from plaques. On the other hand, in another apoE complementation model, the genetic knockdown of CCR7 did not affect regression, and loss of macrophages in the plaque was attributed to reduced monocyte infiltration rather to increased egress[8]. Our results show no difference in monocyte recruitment between WT and MΦLRP1$^{-/-}$ recipient mice (Fig 6F and G). A limitation in our study was the inability to directly track the emigration of EDU labeled monocyte/macrophages from the plaque to the lymph nodes. Thus, use of CCL19/21 blocking antibodies during regression will be necessary to determine whether CCR7 is responsible for the increased egress and subsequent accelerated plaque regression in our study.

The expression of LRP1 in multiple cell types, including macrophages, has been characterized as protective against atheroma formation in murine models of disease progression. Its loss in smooth muscle cells leads to worsened atherosclerosis and formation of aortic aneurysms[44, 45], whereas its loss in macrophages accelerates plaque growth due to decreased M2:M1 plaque macrophage ratios, elevated circulating Ly6C^{hi} monocytes, enhanced susceptibility to apoptosis, and impaired efferocytosis[21,22, 24]. Our finding that loss of macrophage LRP1 accelerates plaque resolution during atherosclerosis regression may be due to the dual role of LRP1 in mediating the effects of TNFα on vascular inflammation and in balancing the effects of CD47 on efferocytosis[39, 40]. Our results open the way for more focused investigations of the molecular pathways controlling arterial wall homeostasis, and is a stark reminder that the biology of plaque regression is regulated by forces that are different and maybe even opposite to those driving plaque formation and growth. Our results show that LRP1 plays a complex role in limiting inflammation and suggest that inflammation resolution may prove detrimental during regressive conditions.

Supplementary Material

Refer to Web version on PubMed Central for supplementary material.

Acknowledgments

We thank Jessica Minnier for her advice on statistical analyses performed in this manuscript.

Sources of Funding

The authors acknowledge the National Institutes of Health (R01 HL057986 to Sergio Fazio; P01 HL 116263 to MacRae Linton; R01 DK109102 and BX002223 to John Stafford) and the National Research Service Award for support (T32 HL094294 to Paul Mueller).

References

1. Napoli C, D'Armientof P, Mancini FP, Postiglione A, Witztum JL, Palumbo G and Palinski W. Fatty streak formation occurs in human fetal aortas and is greatly enhanced by maternal hypercholesterolemia. Intimal accumulation of low density lipoprotein and its oxidation precede monocyte recruitment into early atherosclerotic lesions. J Clin Invest. 1997;100:2680–2690. doi: 10.1172/JCI119813. [PubMed: 9389731]
2. Stary HC. Lipid and macrophage accumulations in arteries of children and the development of atherosclerosis. Am J Clin Nutr. 2000;72:1297S–1306S. [PubMed: 11063472]
3. Nicholls SJ, Puri R, Anderson T, Ballantyne CM, Cho L, Kastelein JJ, Koenig W, Somaratne R, Kassahun H, Yang J, Wasserman SM, Scott R, Ungi I, Podolec J, Ophuis AO, Cornel JH, Borgman M, Brennan DM and Nissen SE. Effect of Evolocumab on Progression of Coronary Disease in Statin-Treated Patients: The GLAGOV Randomized Clinical Trial. JAMA. 2016;316:2373–2384. doi:10.1001/jama.2016.16951. [PubMed: 27846344]
4. Thorngate FE, Rudel LL, Walzem RL and Williams DL. Low levels of extrahepatic nonmacrophage ApoE inhibit atherosclerosis without correcting hypercholesterolemia in ApoE-deficient mice. Arterioscler Thromb Vasc Biol. 2000;20:1939–1945. [PubMed: 10938015]
5. Wientgen H, Thorngate FE, Omerhodzic S, Rolnitzky L, Fallon JT, Williams DL and Fisher EA. Subphysiologic apolipoprotein E (ApoE) plasma levels inhibit neointimal formation after arterial injury in ApoE-deficient mice. Arterioscier Thromb Vasc Biol. 2004;24:1460–1465. doi: 10.1161/01.ATV.0000134297.61979.3c.
6. Raffai RL, Loeb SM and Weisgraber KH. Apolipoprotein E promotes the regression of atherosclerosis independently of lowering plasma cholesterol levels. Arterioscler Thromb Vasc Biol. 2005;25:436–441. doi:10.1161/01.ATV.0000152613.83243.12. [PubMed: 15591220]
7. Williams KJ, Tabas I and Fisher EA. How an artery heals. Circ Res. 2015;117:909–913. doi: 10.1161/circresaha.115.307609. [PubMed: 26541678]
8. Potteaux S, Gautier EL, Hutchison SB, van Rooijen N, Rader DJ, Thomas MJ, Sorci-Thomas MG and Randolph GJ. Suppressed monocyte recruitment drives macrophage removal from atherosclerotic plaques of A poe−/− mice during disease regression. J Clin Inwst. 2011;121:2025–2036. doi:10.1172/JCI43802.
9. Tall AR, Yvan-Charvet L, Terasaka N, Pagler T and Wang N. HDL, ABC transporters, and cholesterol efflux: implications for the treatment of atherosclerosis. Cell Metab. 2008;7:365–375. doi:10.1016/j.cmet.2008.03.001. [PubMed: 18460328]
10. Feig JE, Rong JX, Shamir R, Sanson M, Vengrenyuk Y, Liu J, Rayner K, Moore K, Garabedian M and Fisher EA. HDL promotes rapid atherosclerosis regression in mice and alters inflammatory properties of plaque monocyte-derived cells. Proc Natl Acad Sci U S A. 2011;108:7166–7171. doi: 10.1073/pnas.1016086108. [PubMed: 21482781]
11. Feig JE, Shang Y, Rotllan N, Vengrenyuk Y, Wu C, Shamir R, Torra IP, Fernandez Hernando C, Fisher EA and Garabedian MJ. Statins promote the regression of atherosclerosis via activation of the CCR7-dependent emigration pathway in macrophages. PLoS One. 2011;6:e28534. doi: 10.1371/journal.pone.0028534. [PubMed: 22163030]
12. Trogan E, Feig JE, Dogan S, Rothblat GH, Angeli V, Tacke F, Randolph GJ and Fisher EA. Gene expression changes in foam cells and the role of chemokine receptor CCR7 during atherosclerosis regression in ApoE-deficient mice. Proc Natl Acad Sci U S A. 2006;103:3781–3786. doi:10.1073/pnas.0511043103. [PubMed: 16537455]
13. Leitinger N and Schulman IG. Phenotypic polarization of macrophages in atherosclerosis. Arterioscler Thromb Vasc Biol. 2013;33:1120–1126. doi:10.1161/atvbaha.112.300173. [PubMed: 23640492]
14. Moore KJ and Tabas I. Macrophages in the pathogenesis of atherosclerosis. Cell. 2011;145:341–355. doi:10.1016/j.cell.2011.04.005. [PubMed: 21529710]
15. Tabas I and Bornfeldt KE. Macrophage Phenotype and Function in Different Stages of Atherosclerosis. Circ Res. 2016;118:653–667. doi:10.1161/circresaha.115.306256. [PubMed: 26892964]

16. Feig JE, Vengrenyuk Y, Reiser V, Wu C, Statnikov A, Aliferis CF, Garabedian MJ, Fisher EA and Puig O. Regression of atherosclerosis is characterized by broad changes in the plaque macrophage transcriptome. PLoS One. 2012;7:e39790. doi:10.1371/journal.pone.0039790. [PubMed: 22761902]

17. Llodra J, Angeli V, Liu J, Trogan E, Fisher EA and Randolph GJ. Emigration of monocyte-derived cells from atherosclerotic lesions characterizes regressive, but not progressive, plaques. Proc Natl Acad Sci U S A. 2004;101:11779–11784. doi:10.1073/pnas.0403259101. [PubMed: 15280540]

18. Kristensen T, Moestrup SK, Gliemann J, Bendtsen L, Sand O and Sottrup-Jensen L. Evidence that the newly cloned low-density-lipoprotein receptor related protein (LRP) is the alpha 2-macroglobulin receptor. FEBSLett. 1990;276:151–155.

19. Ishibashi S, Herz J, Maeda N, Goldstein JL and Brown MS. The two-receptor model of lipoprotein clearance: tests of the hypothesis in “knockout” mice lacking the low density lipoprotein receptor, apolipoprotein E, or both proteins. Proc Natl Acad Sci U S A. 1994;91:4431–4435. [PubMed: 8183926]

20. Linton MF, Hasty AH, Babaev VR and Fazio S. Hepatic apo E expression is required for remnant lipoprotein clearance in the absence of the low density lipoprotein receptor. J Clin Invest. 1998;101:1726–1736. [PubMed: 9541504]

21. Overton CD, Yancey PG, Major AS, Linton MF and Fazio S. Deletion of macrophage LDL receptor-related protein increases atherogenesis in the mouse. Circ Res. 2007;100:670–677. doi: 10.1161/01.RES.0000260204.40510.aa. [PubMed: 17303763]

22. Yancey PG, Blakemore J, Ding L, Fan D, Overton CD, Zhang Y, Linton MF and Fazio S. Macrophage LRP-1 controls plaque cellularity by regulating efferocytosis and Akt activation. Arterioscler Thromb Vasc Biol. 2010;30:787–795. doi:10.1161/atvbaha.109.202051. [PubMed: 20150557]

23. Zhu L, Giunzioni I, Tavori H, Covarrubias R, Ding L, Zhang Y, Ormseth M, Major AS, Stafford JM, Linton MF and Fazio S. Loss of Macrophage Low-Density Lipoprotein Receptor-Related Protein 1 Confers Resistance to the Antiatherogenic Effects of Tumor Necrosis Factor-alpha Inhibition. Arterioscler Thromb Vasc Biol. 2016;36:1483–1495. doi:10.1161/atvbaha.116.307736. [PubMed: 27365402]

24. Yancey PG, Ding Y, Fan D, Blakemore JL, Zhang Y, Ding L, Zhang J, Linton MF and Fazio S. Low-density lipoprotein receptor-related protein 1 prevents early atherosclerosis by limiting lesional apoptosis and inflammatory Ly-6Chigh monocytosis: evidence that the effects are not apolipoprotein E dependent. Circulation. 2011;124:454–464. doi:10.1161/circulationaha. 111.032268. [PubMed: 21730304]

25. Tanigawa H, Billheimer JT, Tohyama J, Zhang Y, Rothblat G and Rader DJ. Expression of cholesteryl ester transfer protein in mice promotes macrophage reverse cholesterol transport. Circulation. 2007;116:1267–1273. doi:10.1161/circulationaha.107.704254. [PubMed: 17709636]

26. Zhu L, Brown WC, Cai Q, Krust A, Chambon P, McGuinness OP and Stafford JM. Estrogen treatment after ovariectomy protects against fatty liver and may improve pathway-selective insulin resistance. Diabetes. 2013;62:424–434. doi:10.2337/db11-1718. [PubMed: 22966069]

27. Linton MF, Atkinson JB and Fazio S. Prevention of atherosclerosis in apolipoprotein E-deficient mice by bone marrow transplantation. Science. 1995;267:1034–1037. [PubMed: 7863332]

28. Peled M and Fisher EA. Dynamic Aspects of Macrophage Polarization during Atherosclerosis Progression and Regression. Front ImmunoL 2014;5:579. doi:10.3389/fimmu.2014.00579. [PubMed: 25429291]

29. Xian X, Ding Y, Dieckmann M, Zhou L, Plattner F, Liu M, Parks JS, Hammer RE, Boucher P, Tsai S and Herz J. LRP1 integrates murine macrophage cholesterol homeostasis and inflammatory responses in atherosclerosis. Elife. 2017;6:e29292. doi:10.7554/eLife.29292. [PubMed: 29144234]

30. Feig JE, Parathath S, Rong JX, Mick SL, Vengrenyuk Y, Grauer L, Young SG and Fisher EA. Reversal of hyperlipidemia with a genetic switch favorably affects the content and inflammatory state of macrophages in atherosclerotic plaques. Circulation. 2011;123:989–998. doi:10.1161/CIRCULATIONAHA.110.984146. [PubMed: 21339485]

31. Desurmont C, Caillaud J-M, Emmanuel F, Benoit P, Fruchart JC, Castro G, Branellec D, Heard J-M and Duverger N. Complete Atherosclerosis Regression After Human ApoE Gene Transfer in

ApoE-Deficient/Nude Mice. Arterioscler Thromb Vasc Biol. 2000;20:435–442. doi: 10.1161/01.atv.20.2.435. [PubMed: 10669641]

32. Reis ED, Li J, Fayad ZA, Rong JX, Hansoty D, Aguinaldo JG, Fallon JT and Fisher EA. Dramatic remodeling of advanced atherosclerotic plaques of the apolipoprotein E-deficient mouse in a novel transplantation model.J Vasc Surg. 2001;34:541–547. doi:10.1067/mva.2001.115963. [PubMed: 11533609]
33. Fisher EA. Regression of Atherosclerosis: The Journey From the Liver to the Plaque and Back. Arterioscler Thromb Vasc Biol. 2016;36:226–235. doi:10.1161/atvbaha.115.301926. [PubMed: 26681754]
34. Daugherty A, Tall AR, Daemen M, Falk E, Fisher EA, Garcia-Cardena G, Lusis AJ, Owens AP, 3rd, Rosenfeld ME and Virmani R. Recommendation on Design, Execution, and Reporting of Animal Atherosclerosis Studies: A Scientific Statement From the American Heart Association. Arterioscler Thromb Vasc Biol. 2017;37:e131–e157. doi:10.1161/atv.0000000000000062. [PubMed: 28729366]
35. Fazio S, Babaev VR, Murray AB, Hasty AH, Carter KJ, Gleaves LA, Atkinson JB and Linton MF. Increased atherosclerosis in mice reconstituted with apolipoprotein E null macrophages. Proc Natl Acad Sci U S A. 1997;94:4647–4652. [PubMed: 9114045]
36. Tangirala RK, Tsukamoto K, Chun SH, Usher D, Pure E and Rader DJ. Regression of atherosclerosis induced by liver-directed gene transfer of apolipoprotein A-I in mice. Circulation. 1999;100:1816–1822. [PubMed: 10534470]
37. Zhang Y, Zanotti I, Reilly MP, Glick JM, Rothblat GH and Rader DJ. Overexpression of apolipoprotein A-I promotes reverse transport of cholesterol from macrophages tofeces in vivo. Circulation. 2003;108:661–663. [PubMed: 12900335]
38. Martel C, Li W, Fulp B, Platt AM, Gautier EL, Westerterp M, Bittman R, Tall AR, Chen S-H, Thomas MJ, Kreisel D, Swartz MA, Sorci-Thomas MG and Randolph GJ. Lymphatic vasculature mediates macrophage reverse cholesterol transport in mice. J Clin Inwst. 2013;123:1571–1579. doi:10.1172/JCI63685.
39. Kojima Y, Downing K, Kundu R, Miller C, Dewey F, Lancero H, Raaz U, Perisic L, Hedin U, Schadt E, Maegdefessel L, Quertermous T and Leeper NJ. Cyclin-dependent kinase inhibitor 2B regulates efferocytosis and atherosclerosis. J Clin Inwst. 2014;124:1083–1097. doi:10.1172/jci70391.
40. Kojima Y, Volkmer JP, McKenna K, Civelek M, Lusis AJ, Miller CL, Direnzo D, Nanda V, Ye J, Connolly AJ, Schadt EE, Quertermous T, Betancur P, Maegdefessel L, Matic LP, Hedin U, Weissman IL and Leeper NJ. CD47-blocking antibodies restore phagocytosis and prevent atherosclerosis. Nature. 2016;536:86–90. doi:10.1038/nature18935. [PubMed: 27437576]
41. Xuan W, Qu Q, Zheng B, Xiong S and Fan GH. The chemotaxis of M1 and M2 macrophages is regulated by different chemokines. J Leukoc Biol. 2015;97:61–69. doi:10.1189/jlb.1A0314-170R. [PubMed: 25359998]
42. Llorente-Cortes V, Royo T, Otero-Vinas M, Berrozpe M and Badimon L. Sterol regulatory element binding proteins downregulate LDL receptor-related protein (LRP1) expression and LRP1-mediated aggregated LDL uptake by human macrophages. Cardiovasc Res. 2007;74:526–536. doi: 10.1016/j.cardiores.2007.02.020. [PubMed: 17376415]
43. Lillis AP, Muratoglu SC, Au DT, Migliorini M, Lee MJ, Fried SK, Mikhailenko I and Strickland DK. LDL Receptor-Related Protein-1 (LRP1) Regulates Cholesterol Accumulation in Macrophages. PLoS One. 2015;10:e0128903. doi:10.1371/journal.pone.0128903. [PubMed: 26061292]
44. Boucher P, Gotthardt M, Li WP, Anderson RG and Herz J. LRP: role in vascular wall integrity and protection from atherosclerosis. Science. 2003;300:329–332. doi:10.1126/science.1082095. [PubMed: 12690199]
45. Zhou L, Takayama Y, Boucher P, Tallquist MD and Herz J. LRP1 regulates architecture of the vascular wall by controlling PDGFRbeta-dependent phosphatidylinositol 3-kinase activation. PLoS One. 2009;4:e6922. doi:10.1371/journal.pone.0006922. [PubMed: 19742316]

Clinical Perspective

What is new?

- Our study identifies a macrophage protein, LRP1, whose deletion enhances plaque regression following correction of hyperlipidemia.
- LRP1 expression is reduced in alternatively differentiated macrophages.
- LRP1 absence increases reverse cholesterol transport in vivo.
- SREBP-dependent up-regulation of genes including CCR7 enhances the ability of $LRP1^{-/-}$ macrophages to emigrate from plaques.
- Our results support the notion that plaque regression and progression are under separate regulation.

What are the clinical implications?

- Systemic interventions aimed at controlling plasma glucose, blood pressure, plasma lipids, and inflammation have minimal impact on plaque regression.
- Our studies advance the field by identifying LRP1, a member of the LDLR family, as a player in regulating plaque regression when systemic conditions are kept constant.
- Although LRP1 is not likely to be a therapeutic target, its dual role in mediating inflammation and efferocytosis will improve our understanding of the pathways responsible for plaque regression.

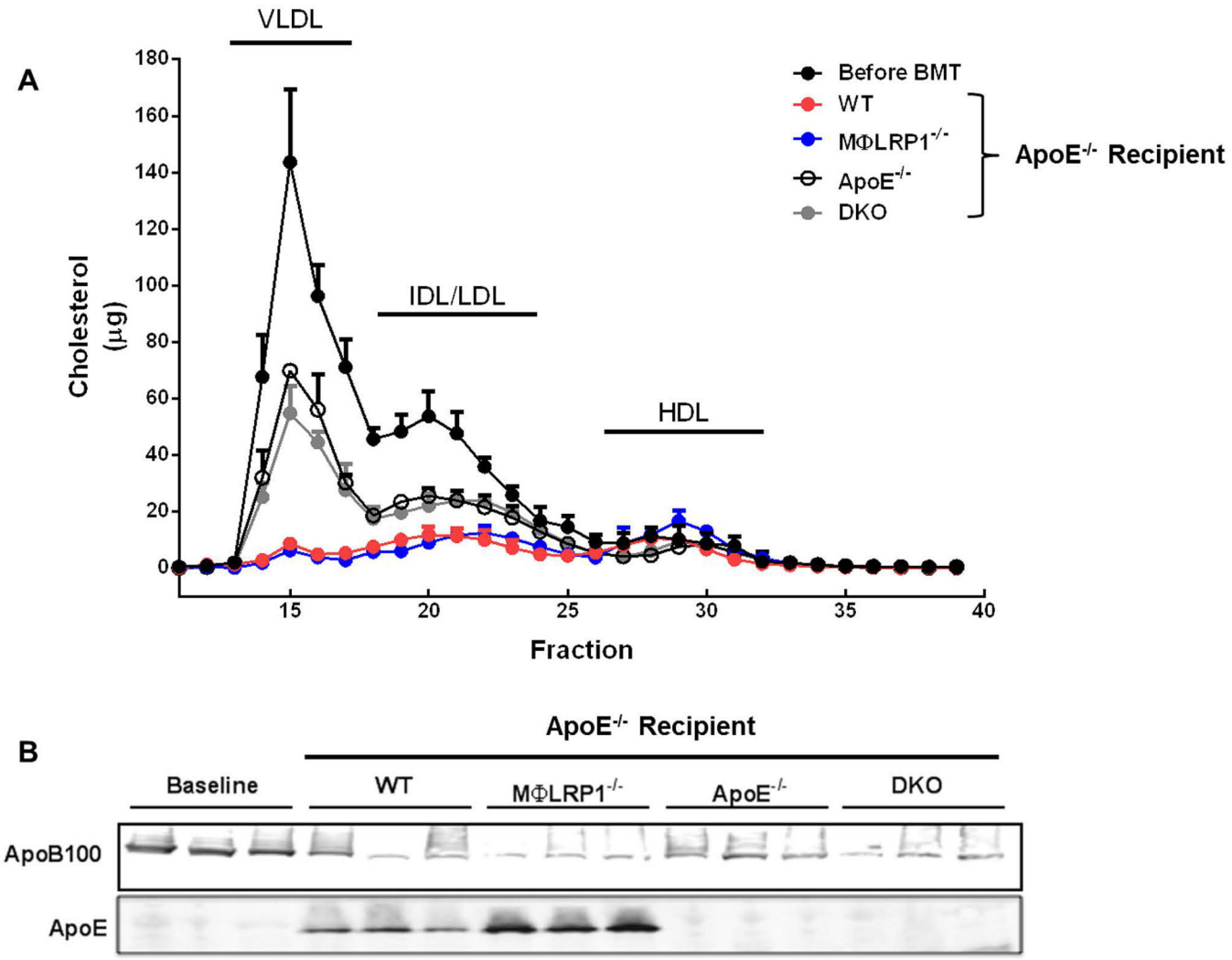

Figure 1. Lipid Profiles in ApoE$^{-/-}$ Mice Undergoing Regression or A rrested Progression.

Serum was collected from apoE$^{-/-}$ mice after 12 weeks on Western diet (Before BMT) and from wildtype (WT), MΦLR1$^{-/-}$, apoE$^{-/-}$, and apoE$^{-/-}$/MΦLRP1$^{-/-}$ (DKO) recipient mice following 10 weeks on chow diet. Pooled serum subjected tofPLC as described in Materials and Methods.(A) Total serum cholesterol(μg) for each fraction. (B) Immunoblot using serum for apoB100 and apoE. Each data point reflects pooled serum from 2–3 mice.

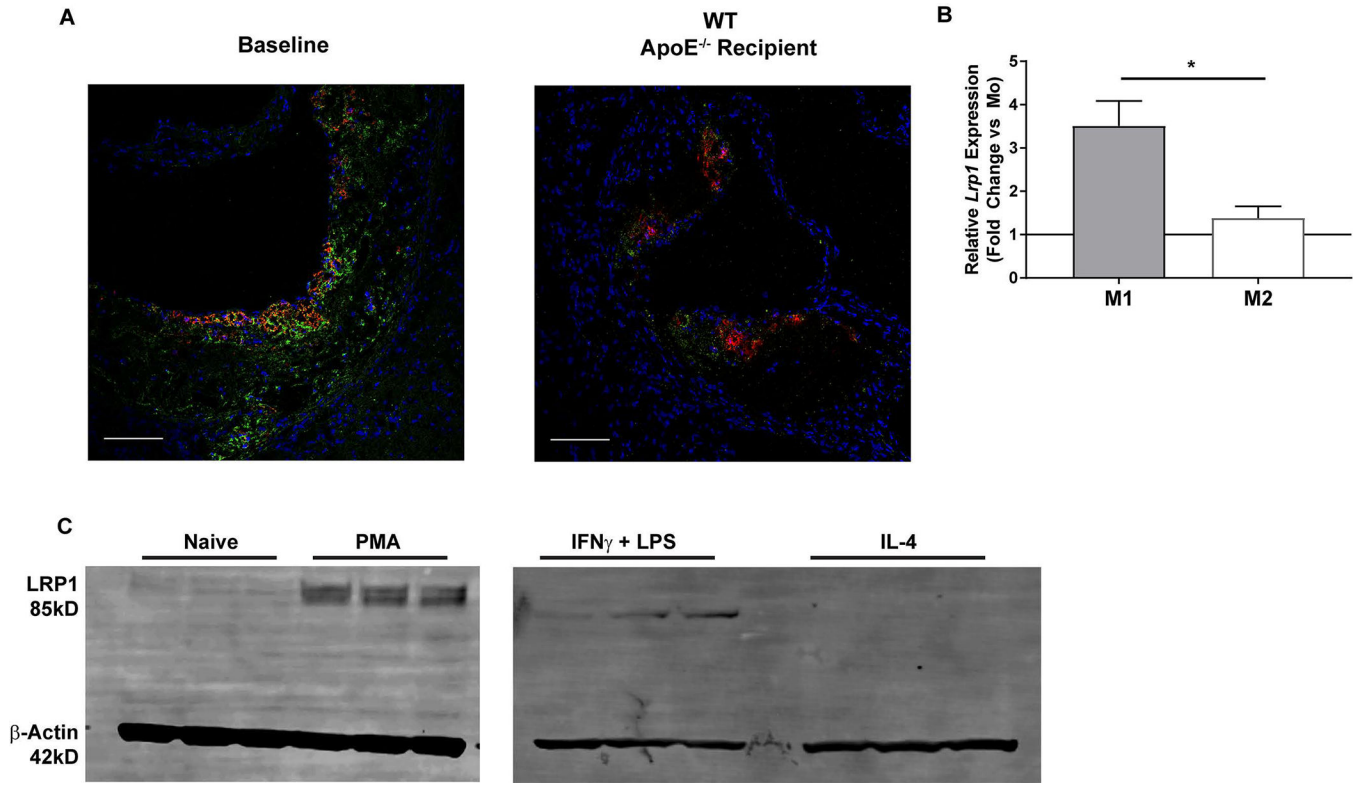

Figure 2. LRP1 expression in the regression of atherosclerosis.

(A) Plaques from baseline and wildtype (WT) recipient mice were stained with DAPI (blue), Mac-2 (red) and LRP1 (green) as described in Materials and Methods. Scale bar = 100μm. (B) Mouse peritoneal macrophages were isolated from WT mice (n=3) and polarized to the M1 or M2 phenotype as described in Materials and Methods. qRT-PCR was used to determine mRNA levels of LRP1 and reported as fold change over the primed controls (Mo) (IFNγ treated only; solid black line). Gene expression data are represented as mean ± SEM and Wilcoxon Signed Rank test was performed to determine differences from Mo. Student's t-test was used to determine differences between genotypes. *P<0.05. (C) THP-1 monocytes were differentiated to macrophages with phorbol 12-myristate 13-acetate (PMA) treatment for 48 hours. Differentiated THP-1 macrophages were then primed with IFNγ for 6–8 hours followed by treatment with either IFNγ and LPS or IL4 for 12 hours as described in Materials and Methods. LRP1 and β-Actin were visualized and quantified via Western blotting.

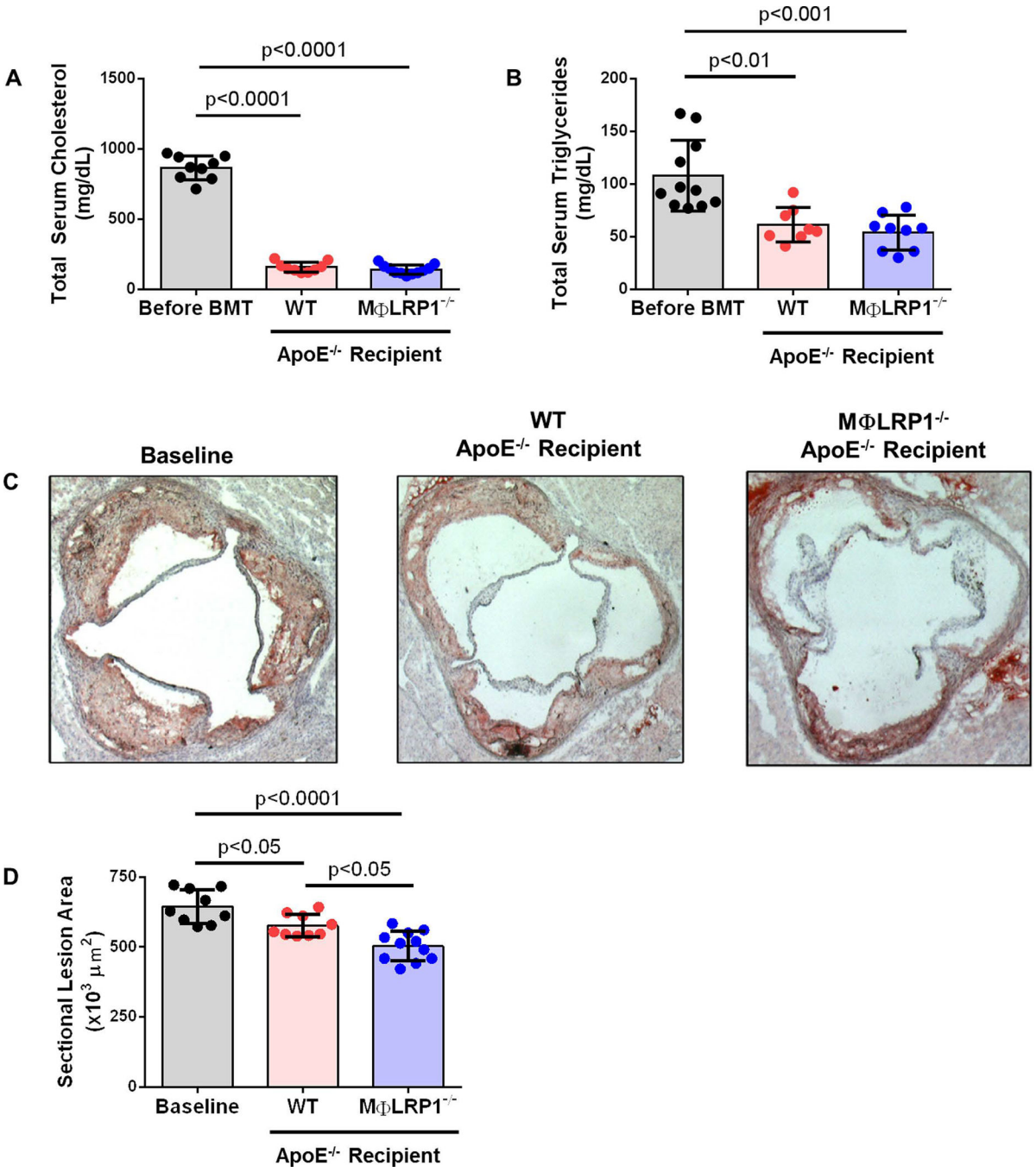

Figure 3. Analysis of Atherosclerosis in Regression.

Atherosclerosis was developed in apoE$^{-/-}$mice as described in Materials and Methods. After lethal irradiation, mice underwent BMT from wildtype (WT) or MΦLRP1$^{-/-}$ mice and switched to chow diet for 10 weeks. ApoE$^{-/-}$ recipient mice were sacrificed after 2 weeks on chow diet and used as baseline. (A) Total serum cholesterol and (B) total serum triglycerides from apoE$^{-/-}$ on Western diet for 12 weeks (Before BMT) and from WT and MΦLRP1$^{-/-}$ recipient mice after 10 weeks on chow diet (mg/dL). (C) and (D) Cross-sections of aortic sinus were obtained and plaque area determined by Oil Red O staining (×10^3 µm^2). One-

way ANOVA with Bonferroni's post hoc tests were used to compare effects across genotypes.

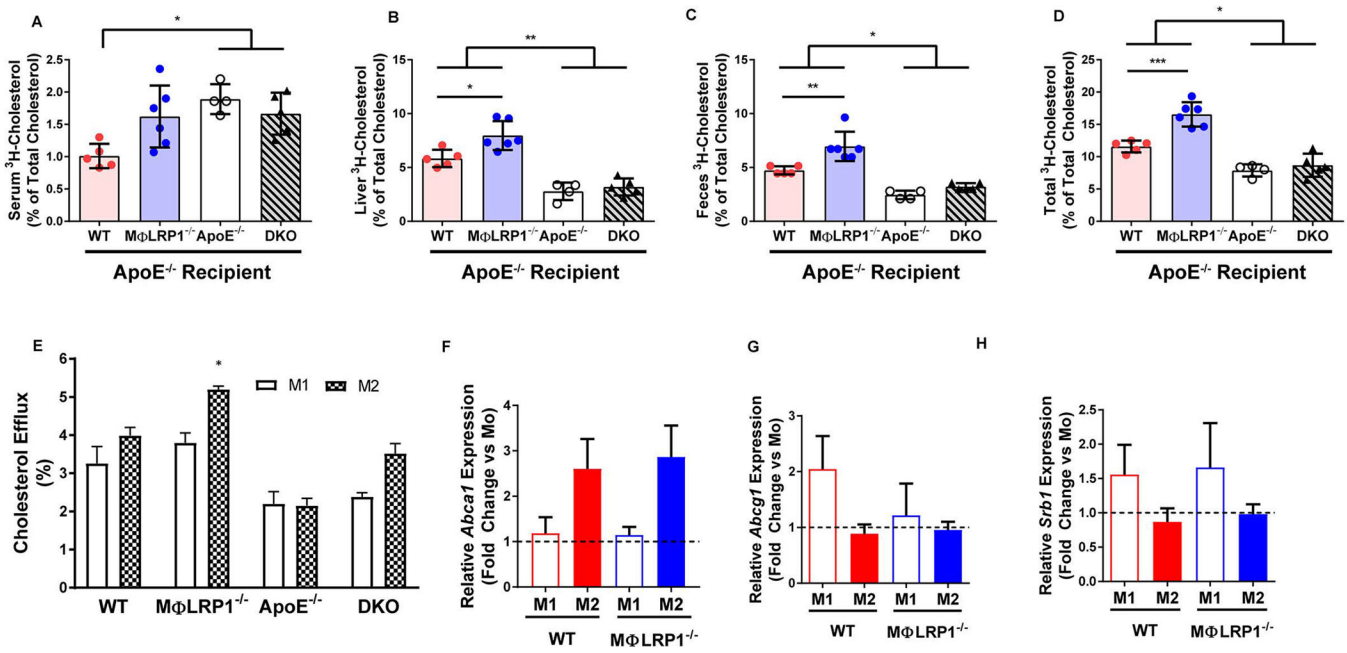

Figure 4. In Vivo and In Vitro Reverse Cholesterol Transport (RCT).

Peritoneal macrophages (MPMs) from wildtype (WT) and MΦLR1$^{-/-}$, apoE$^{-/-}$, and apoE$^{-/-}$/MΦLR1$^{-/-}$(DKO) mice were cultured with acetylated LDL (50 μg/mL) containing ^{3}H-cholesterol for 48 hours. After equilibration, macrophages were injected into mice of their respective donor genotype undergoing regression (chow diet). RCT was determined as described in Materials and Methods. ^{3}H-cholesterol in (A) serum, (B)liver, (C) feces, and (D) total of all three compartments (% of total cholesterol).(E) *In vitro* cholesterol efflux to ApoAl in Ml and M2 MPMs from WT and MΦLR1$^{-/-}$, apoE$^{-/-}$ and DKO mice was determined as described in Materials and Methods. WT and MΦLRP1$^{-/-}$ MPMs were first primed (Mo) and then differentiated to Ml or M2 polarizations as described in Materials and Methods. qRT-PCR was used to determine changes in gene expression of (F) A bcal,(G) Abcgl and (H) Srbl and reported as fold change over IFNγ primed macrophages (Mo; black dashed line). Gene expression data are presented as mean ± SEM. For RCT one-way ANOVA with Bonferroni's post hoc tests were used to compare effects across genotypes. For cholesterol efflux and gene expression, two-way ANOVA with Sidak's multiple comparisons test was used to compare effects across genotypes and macrophage subtypes. ***P<0.001, **P<0.01, *P<0.05.

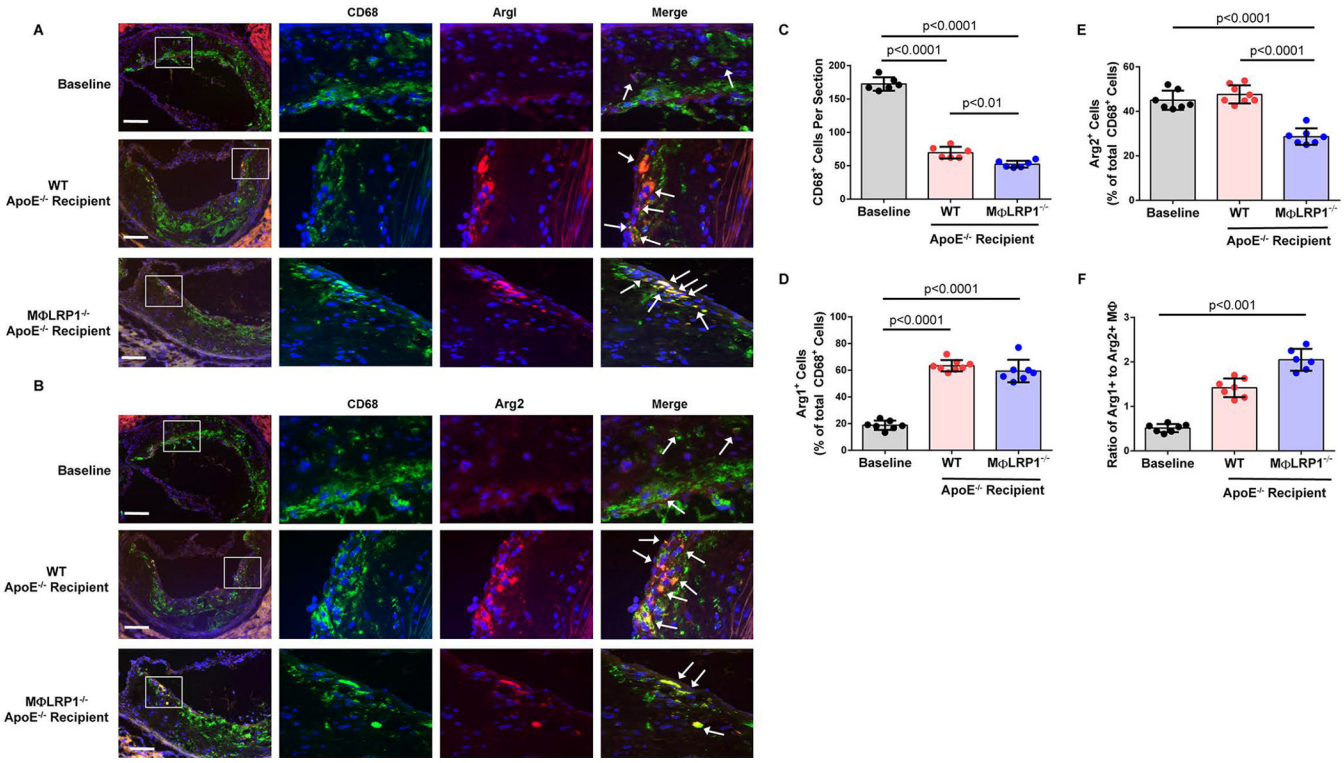

Figure 5. Characterization of Plaque M acrophages During Regression.

Plaques from baseline, wildtype (WT) and MΦLR1$^{-/-}$ recipient mice were stained with DAPI (blue), CD68 (green) and arginase (red) for visualizing macrophages as described in Materials and Methods. Quantification of M2 and M1 macrophages reported as percent of total CD68^{+} cells. Scale bar = 100μm. (A) and (D) M2 macrophages were identified by colocalization of Arg1^{+} and CD68^{+} staining (white arrows). (B) and (E) M1 macrophages were identified as Arg2^{+} and CD68^{+} (white arrows). (C) Quantification of CD68^{+} macrophage cell numbers reported as cells per section. (F) The ratio of M2 (Arg1^{+}) to M1(Arg2^{+}) macrophages in plaques. Kruskal-Wallis test with Dunn's post hoc analysis was performed to determine differences among genotypes. Oneway ANOVA with Bonferroni's post hoc test was used for comparison among all genotypes unless stated otherwise.

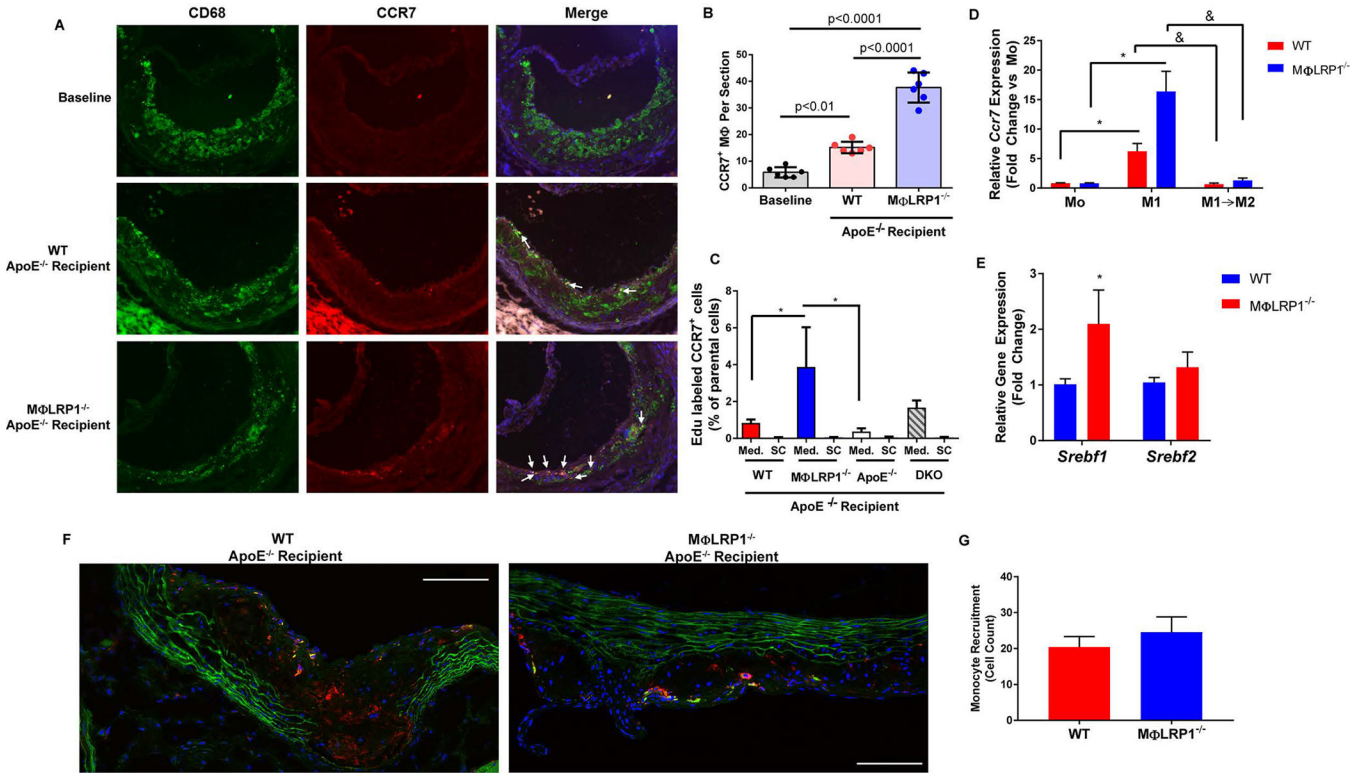

Figure 6. CCR7-dependent Macrophage Egress from Plaques During Regression.

(A) Immunofluorescent staining of CD68 (green), CCR7 (red) and Hoechst (blue) in plaques from baseline and wildtype (WT) and MΦLR1$^{-/-}$ recipient mice undergoing regression. Scale bar = 100μm. (B) Percentage of CD68^{+} CCR7^{+} double positive macrophages (white arrows) relative to total CD68+ macrophage numbers. One-way ANOVA with Bonferroni's post hoc test was used to compare effects among genotypes. (C) EDU-labeled CD11b monocytes from WT, MΦLR1$^{-/-}$, apoE$^{-/-}$ and DKO donor mice were injected into recipient mice of their respective genotype on chow diet (n=4–6 mice/genotype). After 72 hours mice were sacrificed and *in vivo* macrophage egress into the mediastinal lymph nodes (Med.) and superficial cervical control lymph nodes (SC) was determined via FACS analysis of EDU^{+} CCR7^{+} double-positive cells as described in Materials and Methods. ANCOVA was performed to determine differences in Med. lymph nodes using donor genotype as the independent variable and paired SC lymph nodes as the covariate. Tukey's post hoc test was used to determine pairwise differences in Med. lymph nodes. *P<0.05. (D) qRT-PCR was used to determine *Ccr7* expression in mouse peritoneal macrophages (n=5–6/genotype) primed with IFNγ (50ng/mL; Mo) (dark red and dark blue bars) or differentiated to M1 (open bars) or switched from M1 to M2 (pink and light blue bars) as described in Materials and Methods. Data are presented as mean ± SEM and Wilcoxon Signed Rank test was performed to determine differences from Mo (*P<0.05). Unpaired Mann-Whitney test was performed to determined individual differences between groups ($^{\&}$P<0.05). (E) qRT-PCR was used to determine changes in *Srebf1* and *Srebf2* expression in MPMs isolated from WT and MΦLR1$^{-/-}$mice (n=6 and n=5 respectively) and differentiated to the M1 phenotype. Data are represented as mean ± SEM and normalized to the WT recipient group. Unpaired Mann Whitney test was used to compare differences in gene expression between genotypes.

*P<0.05. CD11b monocytes isolated from WT and MΦLR1$^{-/-}$ donor mice were labeled with CMFDA Green Cell Tracker and injected i.v. into WT and MΦLRP1$^{-/-}$ recipient mice (n=3 and n=4 respectively) undergoing regression (2×10^6 monocytes/mouse). After 72 hours, mice were sacrificed and aortic sinus tissue was sectioned. (F) Aortic sinus sections were immunofluorescently stained for CD68 (red) and DAPI (blue) as described in Materials and Methods. Scale bar = 100μm. (G) Monocyte recruitment was determined by counting newly recruited monocyte/macrophages (green) positive for CD68 and normalized to lesion area. Student's t-test was performed to determine differences in monocyte recruitment.